

Quantum Control of the Tin-Vacancy Spin Qubit in Diamond

Debroux, Romain; Michaels, Cathryn P.; Purser, Carola M.; Wan, Noel; Trusheim, Matthew E.; Martínez, Jesús Arjona; Parker, Ryan A.; Stramma, Alexander M.; de Santis, Lorenzo; More Authors

Publication date

2022

Document Version

Final published version

Published in

CLEO

Citation (APA)

Debroux, R., Michaels, C. P., Purser, C. M., Wan, N., Trusheim, M. E., Martínez, J. A., Parker, R. A., Stramma, A. M., de Santis, L., & More Authors (2022). Quantum Control of the Tin-Vacancy Spin Qubit in Diamond. In *CLEO: QELS Fundamental Science, QELS 2022* Article FTh4M.3 (Optics InfoBase Conference Papers). Optica Publishing Group (formerly OSA).

Important note

To cite this publication, please use the final published version (if applicable).
Please check the document version above.

Copyright

Other than for strictly personal use, it is not permitted to download, forward or distribute the text or part of it, without the consent of the author(s) and/or copyright holder(s), unless the work is under an open content license such as Creative Commons.

Takedown policy

Please contact us and provide details if you believe this document breaches copyrights.
We will remove access to the work immediately and investigate your claim.

Green Open Access added to TU Delft Institutional Repository

'You share, we take care!' - Taverne project

<https://www.openaccess.nl/en/you-share-we-take-care>

Otherwise as indicated in the copyright section: the publisher is the copyright holder of this work and the author uses the Dutch legislation to make this work public.

Quantum Control of the Tin-Vacancy Spin Qubit in Diamond

Romain Debroux^{1,*}, Cathryn P. Michaels^{1,*}, Carola M. Purser^{1,3,*}, Noel Wan², Matthew E. Trusheim^{2,4}, Jesús Arjona Martínez¹, Ryan A. Parker¹, Alexander M. Stramma¹, Lorenzo de Santis^{2,5}, Evgeny M. Alexeev^{1,3}, Andrea C. Ferrari³, Dirk Englund², Dorian A. Gangloff¹, and Mete Atatüre¹

¹*Cavendish Laboratory, University of Cambridge,*

JJ Thomson Avenue, Cambridge CB3 0HE, United Kingdom

²*Department of Electrical Engineering and Computer Science, Massachusetts Institute of Technology, Cambridge, Massachusetts 02139, USA*

³*Cambridge Graphene Centre, University of Cambridge, Cambridge CB3 0FA, United Kingdom*

⁴*CCDC Army Research Laboratory, Adelphi, Maryland 20783, USA*

⁵*QuTech, Delft University of Technology, P.O. Box 5046, 2600 GA Delft, Netherlands (8-point type, centered, italicized)*

cm2013@cam.ac.uk

Group-IV colour centres in diamond are a promising light-matter interface for quantum networking devices. We demonstrate multiaxis coherent control of the SnV spin-qubit via an all-optical stimulated Raman drive between the ground and excited states. © 2022 The Author(s)

Diamond stands out as a particularly promising solid state host for scalable fabrication of quantum light-matter interfaces [1]. Within diamond, the group-IV colour centres have demonstrated excellent optical properties [2] and long coherence times at millikelvin temperatures [3]. The negatively charged tin-vacancy center (SnV) is particularly interesting amongst the group-IV colour centres, as its large spin-orbit coupling offers strong protection against phonon dephasing and robust cyclicity of its optical transitions toward spin-photon-entanglement schemes [4]. Conversely, the strong spin-orbit coupling also gives rise to orbital forbidden spin transitions, which has limited microwave based spin control [4] and may necessitate advanced microwave line engineering to achieve fast, coherent control of the SnV spin qubit. In this paper, we demonstrate all-optical multiaxis coherent control of the SnV spin qubit by driving its efficient and coherent optical transitions with microwave modulated laser fields.

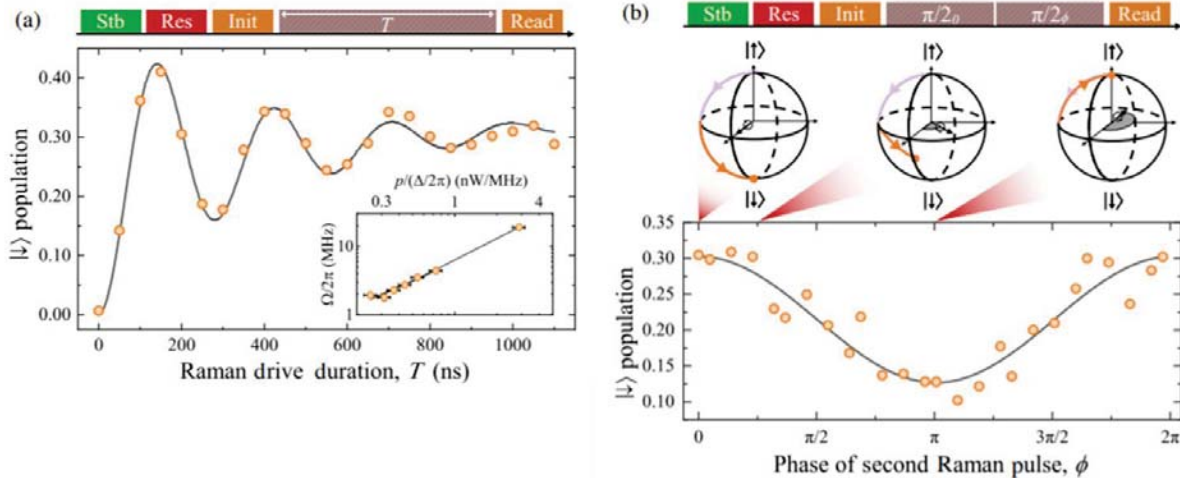


FIG. 1. Multi-axis coherent spin-qubit control. (a) $|\uparrow\rangle$ population (orange circles) as a function of the Raman drive duration T with the pulse sequence shown at the top. The Raman drive is applied with $\Delta/2\pi = 1.2$ GHz and $p = 650(70)$ nW. The black curve is a fit to a two-level model under a master-equation. Inset: $\Omega/2\pi$ as a function of $p/(\Delta/2\pi)$ with a linear fit to the data (solid curve). Here, $\Delta/2\pi$ and p are varied from 300 to 1200 MHz and 40 to 650 nW, respectively. (b) Pulse sequence (top) with one $\pi/2$ pulse about x and a second about an axis rotated by an azimuthal angle ϕ from the x axis. The $\pi/2$ pulse duration is determined from Rabi measurements taken with $\Delta/2\pi = 300$ MHz and $p = 260(30)$ nW. Illustrated on the Bloch spheres are trajectories for $\phi = 0$ (left), $\phi = \pi/4$ (center), and $\phi = \pi$ (right). The $|\downarrow\rangle$ population (orange circles) is plotted as a function of ϕ . The solid curve is a cosine function.

We demonstrate the flexibility of the all-optical approach by implementing, optical Rabi driving (Figure 1), Ramsey interferometry (Figure 2), and dynamical decoupling of the SnV spin qubit (Figure 3).

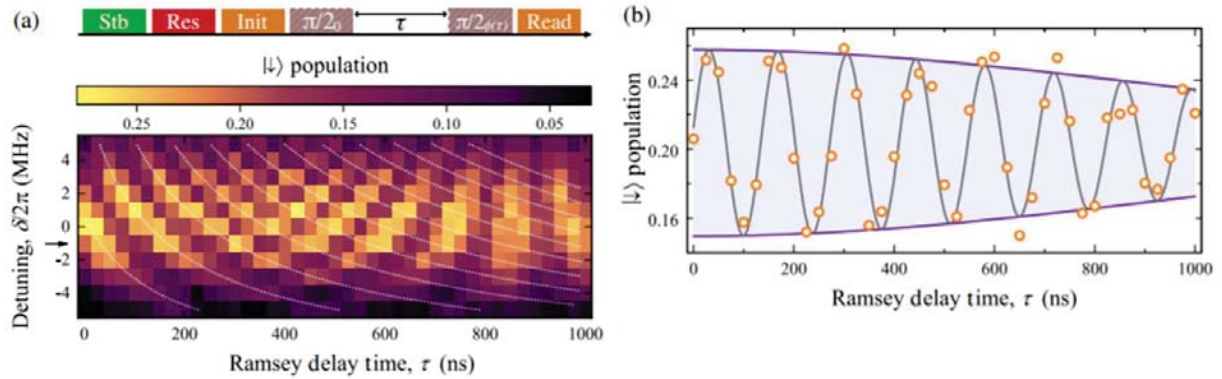


FIG. 2. Ramsey interferometry. (a) Ramsey pulse sequence with two $\pi/2$ pulses separated by a delay time τ (top). The phase of the second pulse is swept according to $\phi = \tau\omega_s$, where $\omega_s/2\pi = 5$ MHz. The color indicates $|\downarrow\rangle$ population plotted as a function of τ and the two-photon detuning, δ . Dotted white curves provide a guide to the eye for the expected $|\downarrow\rangle$ population recovery. (b) Line cut at $\delta/2\pi = -1$ MHz indicated by an arrow in (a), where the $|\downarrow\rangle$ population (orange circles) is measured as a function of τ .

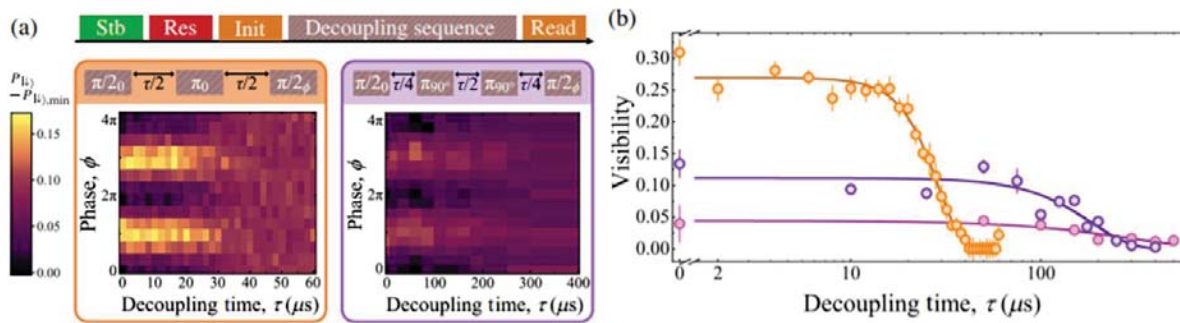


FIG. 3. Dynamical decoupling. (a) Decoupling pulse sequence (top) with two implementations: (left orange panel) Hahn echo, (right purple panel) CPMG-2. The phase ϕ of the second $\pi=2$ pulse is variable. In both panels, color indicates the $|\downarrow\rangle$ population shown as a function of the total decoupling time τ and phase ϕ . (b) Visibility $a=b$ obtained from fitting the function $a \cos(\phi) + b$ to the data shown in (a) at each delay time τ plotted as a function of τ . Hahn echo data (orange circles) are fitted to the function $v_0 \exp[-(\tau/T_2)^n] + v_\infty$, where $v_0 = 0.26(1)$, $v_\infty = 0.013(5)$, $n = 3.7(4)$, and $T_2 = 28.3(6)$ μ s (solid orange curve). CPMG-2 data (purple circles) are fitted to the same function with $v_0 = 0.11(1)$, $n = 2.1(9)$, $T_2 = 0.19(2)$ ms, and v_∞ is fixed to 0 (solid purple curve). CPMG-4 data are plotted (pink circles) and fit to the same function with $v_0 = 0.044(7)$, $n = 1.2(6)$, $T_2 = 0.30(8)$ ms, and v_∞ is fixed to 0 (solid pink curve).

These results confirm the promise of SnV as a competitive next generation light-matter quantum interface and, combined with transform-limited photons [4] and integration into photonic nanostructures [5], our results make the SnV a competitive spin-photon building block for quantum networks.

- [1] M. Atatüre, D. Englund, N. Vamivakas, S. Y. Lee, and J. Wrachtrup, Material platforms for spin-based photonic quantum technologies, *Nat. Rev. Mat.* 3, 38 (2018)
- [2] C. Bradac, W. Gao, J. Forneris, M. E. Trusheim, and I. Aharonovich, Quantum nanophotonics with group IV defects in diamond, *Nat. Commun.* 10, 5625 (2019)
- [3] D. D. Sukachev, A. Sipahigil, C. T. Nguyen, M. K. Bhaskar, R. E. Evans, F. Jelezko, and M. D. Lukin, Silicon-Vacancy Spin Qubit in Diamond: A Quantum Memory Exceeding 10 ms with Single-Shot State Read-out, *Phys. Rev. Lett.* 119, 223602 (2017).
- [4] M. E. Trusheim, B. Pingault, N. H. Wan, M. Gündoğan, L. De Santis, R. Debroux, D. Gangloff, C. Purser, K. C. Chen, and M. Walsh et al., Transform-Limited Photons from a Coherent Tin-Vacancy Spin in Diamond, *Phys. Rev. Lett.* 124, 023602 (2020).
- [5] A. E. Rugar, H. Lu, C. Dory, S. Sun, P. J. McQuade, Z. X. Shen, N. A. Melosh, and J. Vučković, Generation of Tin-Vacancy Centers in Diamond via Shallow Ion Implantation and Subsequent Diamond Overgrowth, *NanoLett.* 20, 1614 (2020).